Available online at www.sciencedirect.com
ScienceDirect
Trans. Nonferrous Met. Soc. China 22(2012) 2831−2839
Transactions of Nonferrous Metals Society of China
www.tnmsc.cn

Thermodynamics of Cr(VI) adsorption on strong alkaline anion exchange fiber

WANG Wen-qing, LI Ming-yu, ZENG Qing-xuan

State Key Laboratory of Explosion Science and Technology,
Beijing Institute of Technology, Beijing 100081, China

Received 19 October 2011; accepted 14 December 2011

Abstract: Removal of Cr(VI) from aqueous solution by strong alkaline anion exchange fiber (SAAEF) was achieved using batch adsorption experiments. The effect of contact time, initial Cr(VI) concentration and pH was investigated. The results showed that the maximum adsorption capacity of SAAEF was 187.7 mg/g at pH=1.0. The adsorption capacity increased with Cr(VI) concentration but decreased with pH value when pH>1.0. Adsorption isotherms at various temperatures were obtained. Langmuir, Freundlich, Dubinin-Radushkevich and Temkin models were adopted and the equilibrium data fitted best with the Langmuir isotherm. The constants of these models indicated that the adsorption process involved both chemisorption and physisorption. The values of thermodynamic parameters, including ΔH, ΔG and ΔS, suggested that the adsorption of Cr(VI) on SAAEF was a spontaneous, entropy-driven and endothermic process. $Q_{(iso)}$ was not a constant value, which indicated an inhomogenous energy distribution on SAAEF.

Key words: strong alkaline anion exchange fiber; hexavalent chromium; isotherm; thermodynamics; chemisorption; physisorption

1 Introduction

Aquatic pollution by heavy toxic metals is a serious environmental problem. Among all the heavy metal ions, Cr(VI) is considered more hazardous to biological systems due to its mutagenic and carcinogenic properties [1]. Cr(VI) could do damage to liver, kidney circulatory and nerve tissues while Cr (III) is much less toxic. Industry discharge of Cr(VI), including mining, textile dyeing, steel fabrication, electroplating, paints and pigments, leather tanning, and chromate preparation [2], is the main source of Cr(VI) pollutants in the last few years [3]. The permissible limit for Cr(VI) is 0.5 mg/L in industrial wastewater [4] while the value is 0.05 mg/L for drinking water by World Health Organization [5].

The conventional method of Cr(VI) removal is the combination of chemical reduction and chemical precipitation. Cr(III) precipitates as $Cr(OH)_3$ at high pH value following the reduction of Cr(VI) to Cr (III). The reductants usually used are $FeSO_4$, $NaHSO_3$ and Na_2SO_3 [6,7]. The residual metal sludge generated easily brings secondary pollution and needs high cost to disposal [8]. Filtration, adsorption, photocatalytic reduction, electrolysis, liquid membrane, ion exchange [9,10], and biological processes based on physical, chemical and biological mechanisms are advisable for Cr(VI) removal. Adsorption is an economic and cost-effective technique with variety of adsorbent materials. Active carbon is the common adsorbent for Cr(VI) removal [2,6,11,12]. A lot of low cost biosorbents including pomace [13], chitosan [8,14], seed pods [15] and some industry wastes have also been studied as Cr(VI) absorbents[16,17]. Low efficiency is the main drawback of adsorption. Membrane, electrochemical treatment performs high efficiency but needs much operational capital. Ion exchange method has many advantages, such as selectivity, recovery of metal value, less sludge volume produced and the meeting of strict discharge specifications [18]. In ion exchange systems, polymeric ion exchange resin (IER) is usually employed. However, IER could be easily poisoned by some organic or inorganic compounds when the pores were clogged by the colloids in the treated solution.

Strong alkaline anion exchange fiber (SAAEF) is a new kind of fabric absorption and separation material. It has higher adsorption/desorption rate and better antipollution ability than ion exchange resin due to the

Foundation item: Project (20080242009) supported by Basic Research Foundation of Beijing Institute of Technology, China
Corresponding author: LI Ming-yu; Tel: +86-10-68915065; Fax: +86-10-68912941; E-mail: mingyuli@163.com
DOI: 10.1016/S1003-6326(11)61539-2

location of function groups [19]. After a number of saturation/regeneration cycles, the fiber is still suitable to further utilization compared with the short life span of IER, which reduces the industrial cost. Besides, there are many application forms of fiber, such as yarn, woven fabric and non-woven fabric. SAAEF has been applied to metal recovery, gas purification and separation, extraction and separation of rare earth and radioactive elements, water purification [20]. Currently, it has also been proposed to use ion-exchange fiber in medical and pharmaceutical applications [21].

In this study, SAAEF was used to the removal of Cr(VI) from aqueous solution. FT-IR spectra before and after adsorption were compared. Factors that affect the adsorption including contact time, initial concentration and pH value were evaluated. Equilibrium isotherm models were applied to obtaining the thermodynamic property and mechanism of Cr(VI) adsorption on SAAEF. Besides, thermodynamic parameters ΔH, ΔG, ΔS and $Q_{(iso)}$ were calculated.

2 Experimental

2.1 Materials

Strong alkaline anion exchange fiber was synthesized by grafting copolymerization of styrene and divinylbenzene onto polypropylene fiber induced by ^{60}co γ-ray co-irradiation followed by chloromethylation and amination [22]. Before the usage, SAAEF was converted to Cl^- type. The chemical structure of SAAEF is shown in Fig. 1.

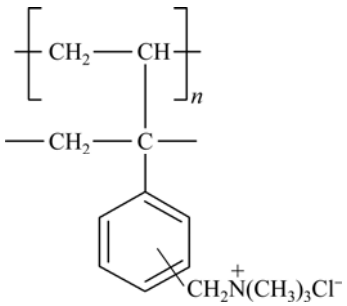

Fig. 1 Chemical structure of SAAEF

Aqueous solution of Cr(VI) was prepared by dissolving potassium dichromate ($K_2Cr_2O_7$) in distilled water. 1,5-diphenylcarbazide ($C_{13}H_{14}N_4O$), acetone, sulfuric acid (95%−98%), and phosphoric acid (≥85%) were used in the analysis of Cr(VI). The initial pH value of Cr(VI) solution was adjusted with sodium hydroxide (NaOH) hydrochloric acid (36%). All reagents used were of chemical grade.

2.2 Equipments

Equipments included electronic scale (AR2140 Ohaus), precision acidity meter (PHS-25 Jingke), mechanical pipettor (20−200 μL Biohit), UV-visible spectrophotometer (725P Apl), water batch oscillator (SHA-B) and Fourier transform infrared spectrometer (TENSOR 27 Bruker).

2.3 Analytical method

The concentration of Cr(VI) was determined by UV-visible spectroscopy using 1,5-diphenylcarbazide as the complexing agent at the wavelength of 540 nm (GB 7467—87). The linear equation of standard curve could be described as

$$A=0.7749+0.0024 \quad (1)$$

where A is the absorbance of the purple colored solution, and c is the concentration of Cr(VI). The correlation coefficient $R^2=0.9999$.

2.4 Adsorption experiment

Adsorption experiments were carried out under batch mode. 20 mL of Cr(VI) aqueous solution with particular initial concentration and pH value was placed in a set of 50 mL glass conical flasks，respectively. Fixed mass of SAAEF was added to the adsorbent solutions. In a water batch oscillator, the mixture of Cr(VI) and SAAEF was agitated at an agitation speed of 120 r/min under a constant temperature for a certain time. The aqueous solution was sampled at predetermined time intervals.

Adsorption capacities at time t, q_t, and equilibrium, q_e, are expressed respectively as

$$q_t=\frac{(c_0-c_t)V}{m} \quad (2)$$

$$q_e=\frac{(c_0-c_e)V}{m} \quad (3)$$

where c_0, c_t and c_e are Cr(VI) the concentrations of original, residual and equilibrium Cr(VI) ion solution, respectively; V is the volume of solution; m is the mass of SAAEF.

2.5 Adsorbent characterization

The characterization of the adsorbent before and after Cr(VI) adsorption was investigated with a Fourier transform infrared spectroscope (FT-IR) in the wave number range of 500−4000 cm^{-1}.

3 Results and discussion

3.1 Characterization of SAAEF

In the FT-IR spectra, 4000−1500 cm^{-1} scope is the characteristic frequency zone, making an assay of some main functional groups, such as O—H, C—H, N—H, C≡C, C≡N, N≡N, C═O, C═N. The zone where

wave numbers below 1500 cm^{-1} called fingerprint region shows some signal bonds and the adsorption peaks are weak. This region reflects subtle changes in molecular structure [23]. The FT-IR spectrum change before and after the adsorption of Cr(VI) on SAAEF is shown in Fig. 2.

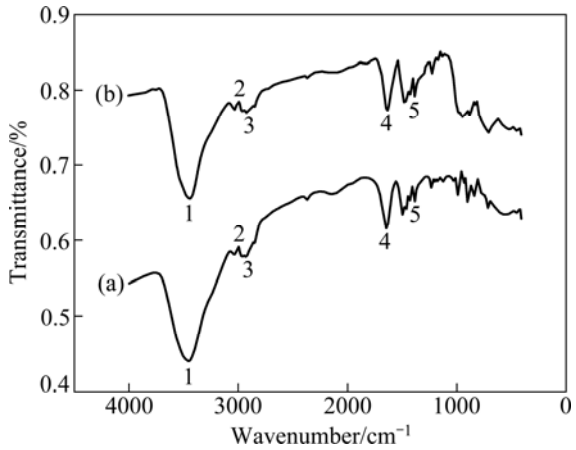

Fig. 2 FT-IR spectra of SAAEF before Cr(VI) adsorption (a) and after Cr(VI) adsorption (b)

The FT-IR spectra in the characteristic frequency region were almost the same before and after the adsorption, indicating that the main functional groups on SAAEF did not change. The main functional groups and the corresponding infrared bands are shown in Table 1. The spectrum change after adsorption appeared in the fingerprint region. The characteristic sorption peaks at 925, 892 and 859 cm^{-1} became strong after the adsorption. This could be explained by the fact that N—C stretch vibration was strengthened after the ion exchange of Cl^- to Cr(VI) ions, making the corresponding bands to be strong.

Table 1 FT-IR spectra characteristics of SAAEF before and after Cr(VI) adsorption

IR peak in Fig. 2	Adsorption band/cm^{-1}		Assignment
	Before adsorption	After adsorption	
1	3454	3442	Bonded —OH groups
2	3026	3025	Benzene C—H stretching
3	2923	2920	—CH_2 groups connected to benzene ring
4	1632, 1513, 1492	1631, 1512, 1471	Benzene ring skeleton stretching
5	1426, 1378	1425, 1375	—CH_3 groups

3.2 Adsorption curve

Adsorption curve expressed in terms of adsorption capacity (q_e) of SAAEF as a function of time (t) is adopted to determine the time of equilibrium. The adsorption curve of SAAEF was carried out (20 mL 483.8 mg/L $K_2Cr_2O_7$, 0.0498 g SAAEF, 294 K, 120 r/min). The results in Fig. 3 show that the adsorption of Cr(VI) onto SAAEF was rather quick and adsorption equilibrium between $K_2Cr_2O_7$ solution and SAAEF almost finished within 10 min, and the increase of Cr(VI) uptake was subtle after 10 min. The adsorption amount of Cr(VI) ions reached a maximum of 187.8 mg/g after 24 h.

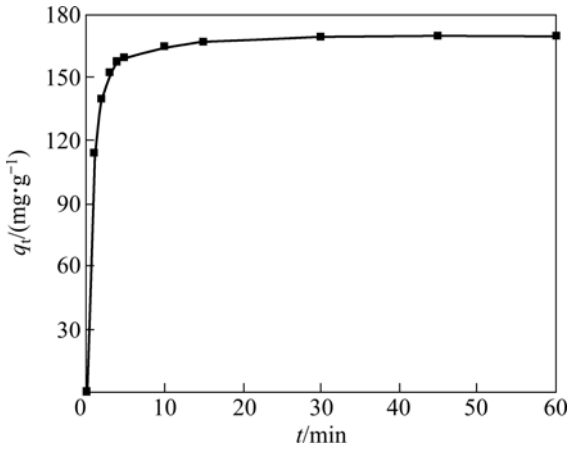

Fig. 3 Effect of time on adsorption

3.3 Effect of Cr(VI) concentration

The effect of Cr(VI) concentration on adsorption was investigated at the chromium concentration of 10−600 mg/L. 0.05 g (±0.0005 g) SAAEF was added to the solution at 303 K. The mixture was agitated at 120 r/min until the adsorption equilibrium.

Figure 4 shows that the adsorption capacity of Cr(VI) increased with increasing initial Cr(VI) concentration and the maximum adsorption capacity of Cr(VI) was 174. 2 mg/g. This could be explained by the fact that increasing the concentration gradient was attributed to the efficiency of Cr(VI) adsorption. Besides, q_e and c_0 fitted a good linear relationship before the platform of adsorption capacity appeared.

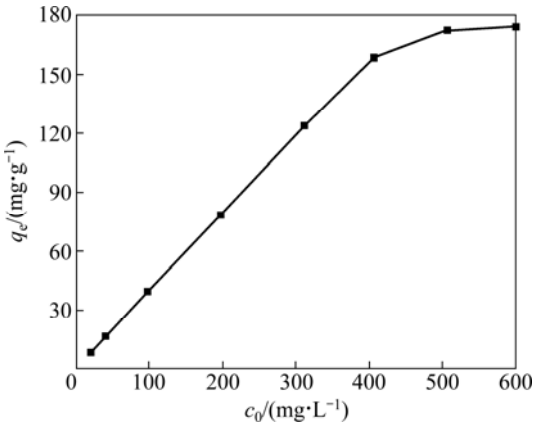

Fig. 4 Effect of Cr(VI) concentration on adsorption

3.4 Effect of pH

The pH value of solution is one of the most important process parameters for the adsorption of metal, especially for the metals whose speciation is governed by the solution acidity. Some experiments were carried out to examine the influence of initial pH on the adsorption of Cr(VI) ions with 600.0 mg/L solutions and 0.05 g (±0.0005 g) SAAEF at 313 K and 120 r/min agitation for 2 h. The initial pH value of the solution was adjusted from 0.50 to 6.50 with HCl or KOH solution.

Figure 5 shows the effect of pH on the Cr(VI) adsorption. SAAEF reached a maximum value of adsorption capacity at pH=1.00. A major drop is observed in removal extent as pH value increases from 1.00 to 6.50. The adsorption capacity of Cr(VI) reduces from 187.7 mg/g to 171.6 mg/g as the pH value increases from 1.00 to 4.00 while the adsorption capacity is stable at about 171.0 mg/g in the pH range of 4.00−5.50. When the pH value is higher than 5.5, the adsorption capacity sharply decreases to 137.8 mg/g at pH=6.50.

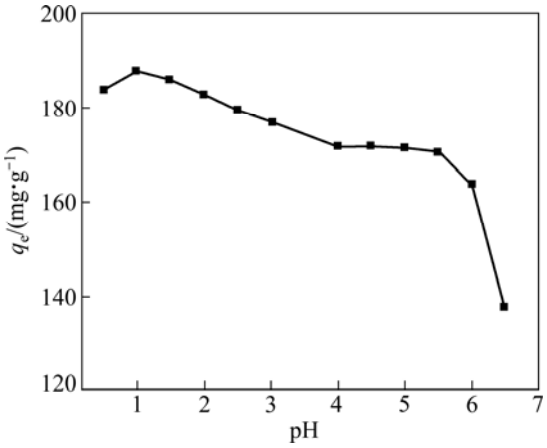

Fig. 5 Effect of pH on adsorption

When the pH value is lower than 1.00, Cr(VI) is present predominantly as $H_2Cr_2O_4$. This molecular form is hindrance to the adsorption based on the fact that the adsorption mechanism of Cr(VI) by SAAEF is ion exchange. With increasing pH value in the range of 1.00−3.00, there exists a mixture of Cr(VI) speciation, including $HCrO_4^-$, $HCr_2O_7^-$, $Cr_3O_{10}^{2-}$ and $Cr_4O_{13}^{2-}$, and decreasing the pH value results in the formation of more polymerised chromium oxide species [24]. Fewer active sites on SAAEF are needed to finish the ion exchange with more polymerised chromium oxide species with the same electric charge, leading to a higher level of Cr(VI) ion uptake. In the pH value range of 3.00−6.00, the speciation of Cr(VI) is stable at $HCrO_4^-$ and $Cr_2O_7^{2-}$ [25], which needs one active site on SAAEF to finish one corresponding Cr(VI) removal. This is in accordance with the experiment data at stable adsorption capacity of 171.0 mg/g. The sharp decrease of adsorption capacity at even higher pH value (pH>5.50) could be explained by the dual competition of the anions to be adsorbed on SAAEF of which OH^- predominates as the availability of OH^- increased.

3.5 Isotherm studies

Equilibrium isotherms at different temperatures for Cr(VI) adsorption on SAAEF experiments were performed at pH=3.0 (20 mL initial Cr(VI) solution of 393.1 mg/L, 0.0400, 0.0430, 0.0450, 0.048, 0.0500, 0.0550, 0.0600, 0.0700, 0.0800 or 0.0900 mg SAAEF, respectively). Figure 6 shows the equilibrium isotherms for Cr(VI) adsorption on SAAEF.

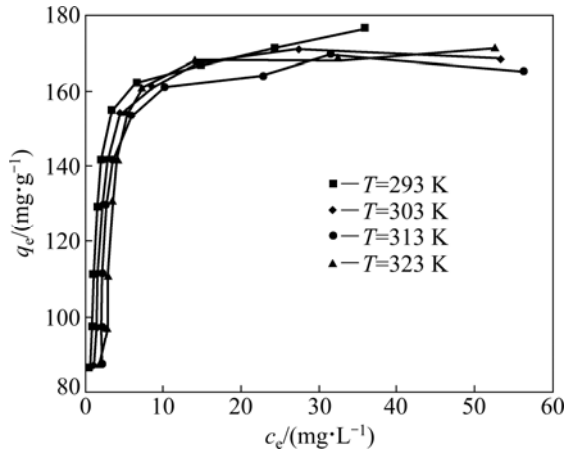

Fig. 6 Adsorption isotherms of Cr(VI)

It can be seen that the isotherm rises in the initial stage with a higher slope at low ρ_e and q_e values until the plateau appears. All the isotherms at various temperatures are close to each other. This indicates that temperature is not a critical factor to Cr(VI) adsorption. The Cr(VI) uptake decreased with temperature. This implies an exothermic process of Cr(VI) adsorption on SAAEF in a temperature range of 293−323 K.

Several adsorption isotherm models, such as Langmuir, Freundlich, Dubinin-Radushkevich and Temkin modle, were employed to describe the adsorption equilibrium between SAAEF and Cr(VI) ion.

3.5.1 Langmuir model

The Langmuir model [26] could be described as

$$q_e = \frac{q_m k_L c_e}{1 + k_L c_e} \tag{4}$$

where c_e is the equilibrium concentration of Cr(VI); q_e and q_m are the equilibrium adsorption amount of Cr(VI) and the saturated monolayer adsorption capacity of Cr(VI) on SAAEF, respectively; k_L is an adsorption equilibrium constant depending on the affinity of binding sites. Equation (5) is transformed to the linear form of the Langmuir equation:

$$\frac{c_e}{q_e}=\frac{1}{q_m k_L}+\frac{c_e}{q_m} \quad (5)$$

Figure 7 displays the fitting lines of the Langmuir equation in all cases. q_m and k_L at each temperature were obtained by the linear regression method and presented in Table 2. The high correlation coefficients (R^2>0.998) and the value of q_m calculated of 178.6 mg/g, which corresponds to the experimental value of 176.7 mg/g, suggest that Langmuir model fitted the sorption data well and the Langmuir equation could be used as the thermodynamic model of Cr(VI) adsorption on SAAEF. Cr(VI) adsorption is a monolayer adsorption process, indicating the chemisorption property between Cr(VI) ion and the active sites on SAAEF. Both q_m and k_L decreased in order of an increase in temperature. This could be explained by the fact that the attraction potential between $Cr_2O_7^{2-}$ and active sites on SAAEF was getting lower, leading to k_L reduction and less Cr(VI) uptake.

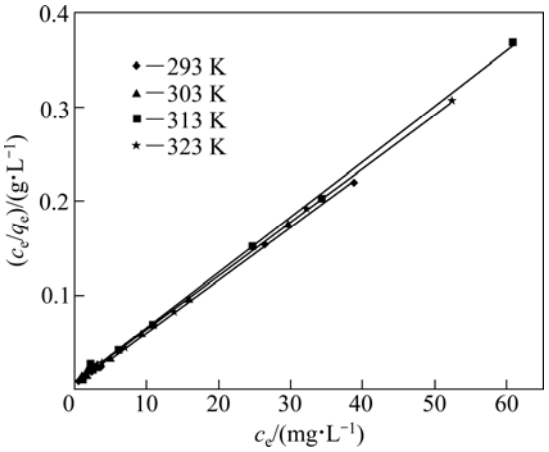

Fig. 7 Langmuir plot for adsorption of Cr(VI) on SAAEF

Another equilibrium parameter or a separation factor, R_L, expresses the essential features of a Langmuir isotherm. The relationships between them are: R_L>1, unfavorable adsorption; R_L=1, linear adsorption; 0<R_L<1, favorable adsorption; R_L=0, irreversible adsorption [27]. R_L is defined as

$$R_L=\frac{1}{1+k_L c_0} \quad (6)$$

where k_L is the Langmuir constant and c_0 is the initial concentration. The calculated values of k_L are included in Table 2. The values of R_L at all temperature are found to be in the range of 0−1, indicating a favorable adsorption of Cr(VI) adsorption on SAAEF and a good performance of SAAEF for the removal of Cr(VI).

3.5.2 Freundlich model

The freundlich model [28] based on multi-molecular layer adsorption on an energy heterogeneous surface is an empirical equation and expressed as

$$q_e=k_F c_e^{1/n} \quad (7)$$

The linear form is

$$\ln q_e=\frac{1}{n}\ln c_e+\ln k_F \quad (8)$$

where k_F and n are the Freundlich constants related to adsorption capacity and intensity, respectively. The slope and the intercept of the line give the values of k_F and n respectively. The maximum sorption capacity (q_m) can be also obtained by the following equation:

$$q_m=k_F c_0^{1/n} \quad (9)$$

where c_0 is the initial concentration of solution. The values of k_F, n, q_m and the correlation coefficients of fitting lines are given in Table 2.

Table 2 Adsorption equilibrium constants obtained from Langmuir and Freundlich isotherms in adsorption of Cr(VI) onto SAAEF

T/K	Langmuir constant				Freundlich constant			
	$k_L/10^{-3}$	q_m/(mg·g^{-1})	$R_L/10^{-3}$	R^2	k_F	n	q_m/(mg·g^{-1})	R^2
293	1363	178.6	1.863	0.9997	109.0	6.350	279.3	0.7729
303	1369	171.8	1.855	0.9997	104.2	6.433	263.8	0.7257
313	911.6	170.0	2.783	0.9988	98.61	6.392	251.1	0.6140
323	816.3	175.7	3.107	0.9990	97.30	5.656	279.8	0.6281

The significant decrement of k_F, n and q_m with the rise in temperature shows the evidence of an exothermic process and values of n larger than 1 show the favorability of adsorption, which agrees with the results from the Langmuir model. However, the maximum q_m value of 279.8 mg/g does not conform to the experimental data and the related coefficient R^2 is lower. Therefore, the experiment data were not well described by the Freundlich equation, which proved that the adsorption of Cr(VI) on SAAEF is not a multi-molecular layer physical adsorption process.

3.5.3 Dubinin-Radushkevich model

Dubinin-Radushkevich [29] equation is another important isotherm model, and the equation is expressed as follows:

$$q_e=q_m\exp(-k\varepsilon^2) \quad (10)$$

After logarithmic transformation, the linear form is

$$\ln\ q_e=\ln\ q_m-k\varepsilon^2 \quad (11)$$

where q_m is the maximum adsorption capacity; k is a constant related to the energy of adsorption; ε is the Polanyi potential, which is calculated from the following equation:

$$\varepsilon = RT\ln(1+\frac{1}{c_e}) \quad (12)$$

where c_e is the retained concentration of solution; R is the mole gas constant; T is the thermodynamic temperature.

The mean free energy of adsorption (E) is calculated using the value of k according to Eq. (12).

$$E=(2k)^{-0.5} \quad (13)$$

The plot of ln q_e versus ε^2 is displayed in Fig. 8. The obtained coefficients of determination (R^2) for the Dubinin-Radushkevich model confirmed a good fit of equilibrium data. The constants k, q_m and E are tabulated in Table 3.

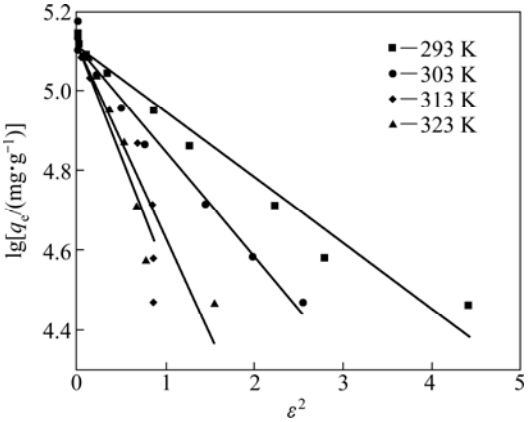

Fig. 8 Dubinin-Radushkevich plot for adsorption of Cr(VI) on SAAEF

The maximum value of q_m regressed from the lines was 168.6 mg/g, which was in proximity with the experimental q_m value of 176.7 mg/g, indicating the applicability of the Dubinin-Radushkevich model to the adsorption of Cr(VI) on SAAEF. The value of E depicted the type of adsorption. When its value is between 8 and 16 kJ/mol, it is an ion exchange adsorption, while it is a physisorption process when E is lower than −40 kJ/mol. The maximum value of E obtained was 1.741 kJ/mol. This suggests that the adsorption of Cr(VI) on SAAEF is not only chemisorption of ion exchange, but also physical adsorption. It is a combination of chemisorption and physical adsorption of Cr(VI) removal.

3.5.4 Temkin model

Temkin model [30] had been established ground on the effects of indirect interactions among adsorbates on adsorption isotherms. The equation of Temkin model is

$$q_e = \frac{RT}{b}\ln Ac_e \quad (14)$$

The linear form of Eq. (14) is

$$q_e = B\ln A + B\ln c_e \quad (15)$$

where $B=RT/b$; T is the thermodynamic temperature; R is the mole gas constant (8.314 J/(mol·K)); A is the equilibrium binding constant corresponding to the maximum binding energy; b is the Temkin constant related to the heat of adsorption.

The constants of the Temkin model were obtained as shown in Table 3. In an ion exchange mechanism, the typical bonding energy range is 8−16 kJ/mol while the value of it is less than −40 kJ/mol in the physisorption processes. The values of b is about 0.10 kJ/mol at all temperatures, which indicates that the adsorption of Cr(VI) on SAAEF involved both chemisorption and physisorption. This is consistent with the result from the Langmuir model. Besides, the values of the Temkin isotherm constant decreased with the temperature, indicating the exothermic nature of Cr(VI) adsorption. However, the related coefficient R^2 is lower compared with the other models.

3.6 Thermodynamic study

The thermodynamic study of Cr(VI) adsorption on SAAEF is critical to the adsorption mechanism. The values of thermodynamic parameters were calculated.

3.6.1 Isometric heat of adsorption $Q_{(iso)}$

$Q_{(iso)}$ is adopted to measure the strength of adsorption. It is the amount of heat release during the adsorption process under a constant temperature. The value of $Q_{(iso)}$ could be measured by calorimeter or calculated by [30]

$$Q_{(iso)} = -R\left.\frac{\mathrm{d}\ln c}{\mathrm{d}(1/T)}\right|_q \quad (16)$$

where c is the retained concentration when the adsorption capacity is q.

The integral form of Eq. (16) can be represented as

$$Q_{(iso)} = 2.303RT_1T_2\left(\frac{\lg c_{e1}-\lg c_{e2}}{T_1-T_2}\right) \quad (17)$$

Table 3 Adsorption equilibrium constants obtained from Temkin and Dubinin-Radushkevich isotherms in adsorption of Cr(VI) on SAAEF

T/K	Dubinin-Radushkevich constant				Temkin constant			
	$k/10^{-3}$	q_m/(mg·g^{-1})	E/(kJ·mol^{-1})	R^2	A	B	b/(J·mol^{-1})	R^2
293	165.2	166.2	1.741	0.9625	196.2	20.91	116.5	0.8379
303	262.9	165.5	1.379	0.9887	166.4	20.43	123.3	0.7844
313	585.6	168.6	0.924	0.8823	110.1	20.61	126.2	0.6824
323	488.1	167.0	1.012	0.9040	59.8	23.31	115.2	0.6872

where T_1 and T_2 are 293 and 313 K, respectively; c_{e1} and c_{e2} are the equilibrium concentrations at T_1 and T_2, respectively.

The values of $Q_{(iso)}$ at different adsorption capacities of Cr(VI) on SAAEF calculated by Eq. (17) are included in Table 4. $Q_{(iso)}$ gets an increase with q_e increasing, which indicates an increase of the coverage ratio of SAAEF surface, and the energy distribution is not homogeneous on the SAAEF. Usually, the value of $Q_{(iso)}$ is more than 42 kJ/mol when a chemisorption takes place while the value is in the range of 0.1−10 kJ/mol in a physisorption process. The value of $Q_{(iso)}$ from 19.11 to 21.41 kJ/(mol·K) which is between the limited $Q_{(iso)}$ values of the two kinds sorption proves that the adsorption of Cr(VI) on SAAEF involved both chemisorption and physisorption.

$Q_{(iso)}$ gets an increase with q_e increasing, which is against the Freundlich and Temkin Models following the fact that $Q_{(iso)}$ decreases with increasing q_e. This explains the bad fitting of the Freundlich and Temkin models using the isotherm data.

3.6.2 Enthalpy change ΔH

ΔH can be obtained by the Clausius-Claoeyron equation represented as [30]

$$\ln c = \frac{\Delta H}{RT} + k \tag{18}$$

where c is the equilibrium concentration; T is the thermodynamic temperature; R is the mole gas constant (8.314 J/(mol·K)); k is a constant. From the isotherms at various temperatures, the adsorption isosteres of ln c_e versus 1/(RT) at different q_e values are displayed in Fig. 9. The values of ΔH were obtained from the slope of the curve.

The negative value of ΔH indicates the exothermic nature of the adsorption. The absolute value of ΔH increases with the increase in temperature, which is in accordance with the change of $Q_{(iso)}$ with temperature alteration.

3.6.3 Gibbs free energy change ΔG

ΔG is usually obtained by the Gibbs equation [30]:

$$\Delta G = -RT\int_0^x q\frac{\mathrm{d}x}{x} \tag{19}$$

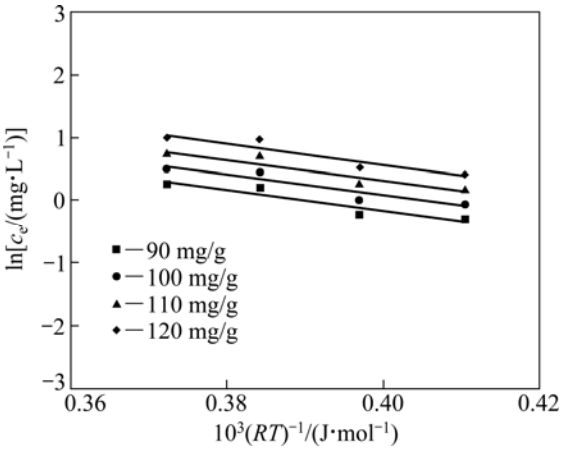

Fig. 9 Plot for lnc_e versus $10^3(RT)^{-1}$

where x is the molar fraction of absorbate; q is the adsorption capacity.

The conversion formula between c and x for Cr(VI) can be expressed as

$$c=3.2\times160x \tag{20}$$

By putting Eqs. (5) and (20) to (19), the integral relation between c and ΔG can be obtained and the values of ΔG are given in Table 4.

The negative and decreased values of ΔG with the increase in temperature reflect that the adsorption of Cr(VI) on SAAEF was a spontaneous process and spontaneity increased with the increase in temperature.

3.6.4 Entropy change ΔS

ΔS can be calculated by Gibbs-Helmholtz equation [31]:

$$\Delta S = \frac{(\Delta H - \Delta G)}{T} \tag{21}$$

where ΔH is the enthalpy change; ΔG is the Gibbs free energy change. The values of ΔS are shown in Table 4.

The values of ΔS are positive, indicating an increase in the randomness at the solid/liquid interface. Besides, the values of ΔS increase with increasing temperature, suggesting that the degree of randomness increase getting larger [32].

Table 4 Thermodynamic parameters for adsorption of Cr(VI) on SAAEF

q_e/(mg·g)	$Q_{(iso)}$/(kJ·mol^{-1})	ΔH/(kJ·mol^{-1})	ΔG/(kJ·mol^{-1})				ΔS/(J·mol^{-1}·K^{-1})			
			293 K	303 K	313 K	323 K	293 K	303 K	313 K	323 K
90	19.11	−16.54	−15.47	−15.67	−15.57	−13.78	4.210	4.256	5.557	5.571
100	19.67	−16.70	−15.47	−15.67	−15.57	−13.78	4.936	5.014	6.448	6.416
110	20.41	−16.92	−15.47	−15.67	−15.57	−13.78	5.761	5.885	7.457	7.350
120	21.41	−17.21	−15.47	−15.67	−15.57	−13.78	6.723	6.907	8.626	8.414

4 Conclusions

1) SAAEF was found effective in the removal of Cr(VI) from aqueous solution and the maximum adsorption capacity reached 187.7 mg/g under optimal conditions.

2) FT-IR spectra suggest that the main functional groups on SAAEF did not change after the adsorption and the ion exchange took place on the surface of SAAEF.

3) The maximum adsorption capacity of Cr(VI) could be obtained at pH=1.0 and it increased with Cr(VI) concentration. The effect of temperature on the adsorption is unobvious.

4) The langmuir, Freundlich, Dubinin-Radushkevich, Temkin modles were adopted to describe the adsorption equilibrium isotherm data, respectively. Among all these models, the Langmuir and the Dubinin-Radushkevich models are in good agreement with the experimental data with high R^2 and reasonable calculated parameters.

5) The values of all the isotherm model constants indicate a favorable adsorption of Cr(VI) on SAAEF and an adsorption process involved both chemisorption and physisorption.

6) The values of thermodynamic parameters were calculated. The energy distribution on SAAEF is inhomogenous because $Q_{(iso)}$ is not a constant value. The negative values of ΔH, ΔG and positive ΔS suggest that the adsorption of Cr(VI) on SAAEF is a spontaneous, entropy-driven and endothermic process.

Acknowledgement

Many experiments were carried out by the assistance of WANG Yong.

References

[1] ZHANG Run-hu, WANG Bo, MA Hong-zhu. Studies on chromium (VI) adsorption on sulfonated lignite [J]. Desalination, 2010, 255: 61−66.

[2] ZHANG Hong, TANG Yi, CAI Dong-qing, LIU Xian-an, WANG Xiang-qin, HUANG Qing, YU Zeng-liang. Hexavalent chromium removal from aqueous solution by algal bloom residue derived activated carbon: Equilibrium and kinetic studies [J]. Journal of Hazardous Materials, 2010, 181: 801−808.

[3] NATALE F D, LANCIA A, MOLINO A, MUSMARRA D. Removal of chromium ions from aqueous solutions by adsorption on activated carbon and char [J]. Journal of Hazardous Materials, 2007, 145: 381−390.

[4] NRIAGU J O, PACYNA J M. Quantitative assessment of worldwide contamination of air, water and soils by trace metals [J]. Nature, 1988, 333(6169): 134−139.

[5] World Health Organization. Guidelines for drinking-water quality [R]. 3rd ed. Geneva, 2004, 1: 334.

[6] OWLAD M, AROUA M K, DAUD W M A W. Hexavalent chromium adsorption on impregnated palm shell activated carbon with polyethyleneimine [J]. Bioresource Technology, 2010, 101: 5098−5103.

[7] EARY L E, RAI D. Chromate removal from aqueous wastes by reduction with ferrous ion [J]. Environmental Science and Technology, 1988, 22: 972−977.

[8] ANDIN Y A, AKSOY N D. Adsorption of chromium on chitosan: Optization, kinetics and thermodynamics [J]. Chemical Engineering Journal, 2009, 151: 188−194.

[9] RENGARAJ S, VENKATARAJ S, YEON JEI-WON, KIM YOUNGHUN, LI X Z, PANG G K H. Preparation, characterization and application of Nd−TiO_2 photocatalyst for the reduction of Cr(VI) under UV light illumination [J]. Applied Catalysis B, 2007, 77: 157−165.

[10] HU Xin-jiang, WANG Jing-song, LIU Yun-guo, LI Xin, ZENG Guang-ming, BAO Zheng-lei, ZENG Xiao-xia, CHEN An-we, LONG Fei. Adsorption of chromium (VI) by ethylenediamine-modified cross-linked magnetic chitosan resin: Isotherms, kinetics and thermodynamics [J]. Journal of Hazardous Materials, 2011, 185: 801−808.

[11] NATALE F DI, LANCIA A, MOLINO A, MUSMARRA D. Removal of chromium ions from aqueous solutions by adsorption on active carbon and char [J]. Journal of Hazardous Materials, 2007, 145: 381−390.

[12] DEMIRAL H, DEMIRAL I, TUMSEK F, KARABACAKOGLU B. Adsorption of chromium (VI) from aqueous solution by activated carbon derived from olive bagasse and applicability of different adsorption models [J]. Chemical Engineering Journal, 2008, 144: 188−196.

[13] MALKOC E, NUHOGLU Y, DUNDAR M. Adsorption of chromium (VI) on pomace—An olive oil industry waste: Batch and column studies [J]. Journal of Hazardous Materials B, 2006, 138: 142−151.

[14] BARONI P, VIEIRA R S, MENEGHETTI E, MENEGHETTI, da SILVA M G C, BEPPU M M. Evaluation of batch adsorption of chromium ions on natural and crosslinked chitosan membranes [J]. Journal of Hazardous Materials, 2008, 152: 1155−1163.

[15] LEVANKUMAR L, MUTHUKUMARAN V, GOBINATH M B. Batch adsorption and kinetics of chromium (VI) removal from aqueous solutions by Ocimum americanum L. seed pods [J]. Journal of Hazardous Materials, 2009, 161: 709−713.

[16] GUPTA V K, RASTOGI A, NAYAK A. Adsorption studies on the removal of hexavalent chromium from aqueous solution using a low cost fertilizer industry waste material [J]. Journal of Colloid and Interface Science, 2010, 342: 135−141.

[17] ANANDKUMAR J, MANDAL B. Adsoption of chromium (VI) and Rhodamine B by surface modified tannery waste: Kinetic, mechanistic and thermodynamic studies [J]. Journal of Hazardous Materials, 2011, 186: 1088−1096.

[18] RENGARAJ S, YEON K H, MOON S H. Removal of chromium from water and wastewater by ion exchange resins [J]. Journal of Hazardous Materials B, 2001, 87: 273−287.

[19] WANG Zhao-yang. Preparation, application and prospect of ion exchange fibers [J]. New Chemical Materials, 2004, 32(6): 27−29. (in Chinese)

[20] ZHOU Shao-ji. The progress of preparation performance and application of chemical adsorbtive fibers [J]. Ion Exchange and Adsorption, 2004, 20(3): 278−288. (in Chinese)

[21] VUORIO M, MANZANARES J A, MURTOMAKI L, HIRVONEN J, KANKKUNENA T, KONTTURI K. Ion-exchange fibers and drugs: A transient study [J]. Controlled Release, 2003, 91(3): 439−448.

[22] LI Ming-yu, ZENG Qing-xuan, FENG Chang-gen, SUN Wei-na, LI Kai. Structure and properties of the strong alkaline anion exchange fiber [J]. Materials Science & Technology, 2006, 14(1): 32−35. (in Chinese)

[23] SU K M, PAN T Y, ZHANG L Y. Spectral analysis methods [M]. Shanghai: East China University of Science and Technology Press, 2002.
[24] PEHLIVAN E, CETIN S. Sorption of Cr(VI) ions on two Lewatit-anion exchange resins and their quantitative determination using UV-visible spectrophotometer [J]. Journal of Hazardous Material, 2009, 163: 448−453.
[25] KARTHIKEYAN T, RAJGOPAL S AND MIRANDA L R. Chromium (VI) adsorption from aqueous solution by hevea brasilinesis sawdust activated carbon [J]. Journal of Hazardous Material B, 2005, 124: 192−199.
[26] LANGMUIR I. The constitution and fundamental properties of solids and liquids [J]. Am Chem Soc, 1916, 38: 2221−2295.
[27] HALL K R, EAGLETON L C, ACRIVOS A, VERMEULEN T. Pore and solid-diffusion kinetics in fixed-bed adsorption under constant pattern conditions [J]. Ind Eng Chem Fundam, 1966, 5: 212−223.
[28] FREUNDLICH H M F. Uber die adsorption in losungen [J]. Zeitsch Phys Chem, 1906, 57: 385−470.
[29] TAN I A W, HAMEED B H, AHMAD A L. Equilibrium and kinetic studies on basic dye adsorption by oil palm fiber activated carbon [J]. Chemical Engineering Journal, 2007, 127: 111−119.
[30] FU Xian-cai, SHEN Wen-xia, YAO Tian-yang, HOU Wen-hua. Physical chemistry [M]. Beijing: Higher Education Press, 2006. (in Chinese)
[31] MEENA A K, KADIRVELU K, MISHRA G K, RAJAGOPAL C, NAGAR P N. Adsorptive removal of heavy metals from aqueous solution by treated sawdust [J]. Journal of Hazardous Material, 2008, 150: 604−611.
[32] NGAH W S W, FATINATHAN S. Adsorption of Cu (II) ions in aqueous solution using chitosan beads, chitosan-GLA beads and chitosan-alginate beads [J]. Chemical Engineering Journal, 2008, 143: 62−72.

强碱性离子交换纤维吸附 Cr(VI)的热力学

王文庆，李明愉，曾庆轩

北京理工大学 爆炸科学与技术国家重点实验室，北京 100081

摘　要：通过静态吸附实验，采用强碱性离子交换纤维(SAAEF)去除水溶液中的 Cr(VI)。分别研究了时间、Cr(VI)的初始浓度和 pH 对该吸附过程的影响。SAAEF 的最大饱和吸附量为 187.7 mg/g(pH=1)。饱和吸附量随着 Cr(VI)浓度的升高而增大，在 pH>1 的酸度范围内，随着 pH 值的增高而减少。采用 Langmuir、Freundlich、Dubinin-Radushkevich 和 Temkin 4 种热力学模型对不同温度的等温吸附曲线进行拟合，结果表明，Langmuir 等温吸附模型是描述 SAAEF 吸附 Cr(VI)热力学过程的最佳模型；模型参数表明，SAAEF 吸附 Cr(VI)的过程既存在物理吸附又存在化学吸附。热力学参数ΔH、ΔG 和ΔS 表明，该吸附过程为一放热、熵增的自发过程。热力学参数$Q_{(iso)}$不为常量，表明 SAAEF 表面存在能量分布不均匀的现象。

关键词：强碱性离子交换纤维；等温吸附线；热力学；化学吸附；物理吸附

(Edited by YANG Hua)